

X-ray Analysis of NiCr_xFe_{2-x}O₄ Nanoparticles Using Debye- Scherrer, Williamson-Hall and Size-strain Plot Methods

I.P. Yaremiy¹, V.S. Bushkova^{1,*}, N.I. Bushkov¹, S.I. Yaremiy²

¹ *Vasyl Stefanyk Precarpathian National University, 57, Shevchenko St., 76025 Ivano-Frankivsk, Ukraine*

² *Ivano-Frankivsk National Medical University, 2, Halytska St., 76018 Ivano-Frankivsk, Ukraine*

(Received 27 February 2019; revised manuscript received 07 August 2019; published online 22 August 2019)

The aim of this work is to create and study NiCr_xFe_{2-x}O₄ nanoparticles using sol-gel technology with participation of auto-combustion (SGA). After completing the auto-combustion process, the phase which corresponds to the cubic structure of spinel space group *Fd3m* was obtained. The dependences of the lattice parameter and X-ray density of the ferrite powders on the nickel content were found. The values of the lattice parameter decrease from 0.8343 nm to 0.8306 nm with an increase in Cr³⁺ ions content. The decrease in lattice parameters by increasing Cr concentration can be attributed to replacement of the bigger ionic radius of Fe³⁺ by smaller ionic radius of Cr³⁺. The X-ray density d_x increases from 5.360 g cm⁻³ to 5.387 g cm⁻³ with increasing degree of substitution x . The cation distribution study indicates that nickel and chromium ions have a tendency to occupy octahedral sites, whereas iron ions have a tendency to occupy both tetrahedral and octahedral sites. Morphological observations reveal that the particle size decreases significantly with increasing Cr content mean while the particle size becomes more uniform. The dimension of the particles and micro-deformations of crystal lattice was calculated from width of X-ray profile and angle. The integral width of K α_1 -line was getting by division the integral width of the K α -doublet obtained from the experiments on coefficient K. The ignoring a doublet in determining the integral width leads to increase of the calculated block sizes by 6 %. The particle size of NiCr_xFe_{2-x}O₄ powders was analyzed by the Scherrer formula, Williamson-Hall and the SSP methods. In determining particle average size by the Williamson-Hall method (24-43 nm), there is a larger scatter of experimental points on the straight line than by the SSP method (19-42 nm). The substitution of Cr³⁺ ions resulted in decrease of nanoparticle sizes. The values of micro-deformations ε obtained using the SSP method are within the range of $4.69 \cdot 10^{-4}$ to $2.69 \cdot 10^{-3}$. The average particle size of NiFe₂O₄ was found from the least-square fit of the lognormal distribution to the measured points obtained by the SEM micrographs. This average particle size was found in the range 41-42 nm.

Keywords: Ferrite, Nanopowder, Sol-gel auto-combustion, X-ray analysis, Micro-deformation.

DOI: [10.21272/jnep.11\(4\).04020](https://doi.org/10.21272/jnep.11(4).04020)

PACS numbers: 75.50.Tt, 81.07.Wx, 61.72.Dd

1. INTRODUCTION

In recent years, the growth of interest in nanodispersed ferrites has stimulated a significant surge of activity in the study of their structure [1]. First of all, the method of electron microscopy, electron diffraction, and other spectroscopic methods give a lot of information on the structure of materials. However, the X-ray diffraction method is the most important method for determining the atomic structure. This method allows the establishment of such important characteristics of nanocrystals as the size of the crystalline blocks, the degree of distortion of the crystalline structure. At present, methods of X-ray analysis are actively developing in application to nanocrystalline materials.

The methods of studying the real structure of polycrystals based on the analysis of the displacement, expansion and form of individual diffraction reflexes are widely used [2, 3] to determine the average sizes of nanoparticles, the parameters of size distribution and the magnitudes of micro-deformations. Methods of full-profile analysis allow to specify the atomic structure of nanoparticles and simultaneously receive information about their size and form.

It is known that a crystal of infinite dimensions in all directions has an ideal structure. Since, in practice, the crystals have finite dimensions, so they cannot be

perfect. The deviation from ideal crystallinity leads to the expansion of diffraction reflexes. The size of the coherent scattering regions (CSRs) and the micro-deformations of the crystal lattice can be defined by analyzing the width of the diffraction reflexes. As a rule, the size of crystallites does not always coincide with the size of powder particles due to the formation of polycrystalline aggregates [4]. Generally, the lattice deformation occurs due to defects in the crystal lattice, for example, through point defects, dislocations. There are other sources of deformation, which include grain boundaries, agglomerations of particles, and others [5]. The size of the crystallites and the deformation of the crystal lattice have a different effect on the Bragg peak. The first parameter increases the width of the reflex, and the second – shifts its position. The line displacement is the basis of the X-ray method for the determination of micro-deformations.

Thus, particle size and morphology play important roles in the applications, which drive the modern studies to focus on the synthesis of new nanocrystalline materials. The structure, mechanical, magnetic, optical, electrical, and dielectric properties of ferrites are dependent upon several factors including the method of preparation, sintering time and temperature, chemical composition, type and amount of dopant [6, 7]. In nickel ferrite, half of the ferric ions preferentially fill the tet-

* bushkovavira@gmail.com

rahedral sites (A), and the other ions occupy the octahedral sites (B) [8]. The Cr^{3+} ions cause appreciable changes in the structural, electrical and magnetic properties [9]. In the present work, the SGA synthesis and structure of nickel-chromium ferrite particles are described using Debye-Scherrer formula, Williamson-Hall and SSP methods.

2. MATERIALS AND METHODS

The nickel-chromium ferrites $\text{NiCr}_x\text{Fe}_{2-x}\text{O}_4$ ($x = 0.0, 0.1, 0.2, 0.3, 0.4$ and 0.5) have been prepared by SGA technique [9]. Using Dron 7 X-ray diffractometer, the X-ray diffraction patterns were recorded at room temperature. The morphology of Ni-Cr ferrites was observed by means of scanning electron microscopy (SEM) with a Hitachi S-4700 electron microscope operating at 20.0 kV.

3. RESULTS AND DISCUSSION

3.1 X-ray Diffraction (XRD)

X-ray diffraction line profile analysis is conventionally used to study the physical and microstructural parameters of polycrystalline materials. X-ray diffraction patterns of nickel-chromium ferrite powders are shown in Fig. 1. For all samples, the analysis of XRD patterns revealed the formation of single phase cubic structure of spinel space group $Fd\bar{3}m$.

Lattice constant of $\text{NiCr}_x\text{Fe}_{2-x}\text{O}_4$ was determined from X-ray data analysis. The values of the lattice parameter decrease from 0.8343 nm to 0.8306 nm with an increase in chromium content. The results are in good agreement with Lee et al. [10]. The decrease in lattice parameters by increasing Cr concentration can be attributed to replacement of the bigger ionic radius of Fe^{3+} (0.0645 nm) by the smaller ionic radius of Cr^{3+} (0.063 nm) [11]. The lattice parameters, X-ray density d_x , molar mass, and cation distribution by sub-lattices of spinel for the $\text{NiCr}_x\text{Fe}_{2-x}\text{O}_4$ powders are given in Table 1. The calculated X-ray density is in the range 5.36-5.39 g/cm^3 . The cation distribution obtained from XRD study indicates that nickel and chromium ions have a tendency to occupy octahedral [B] sites, whereas iron ions have a tendency to occupy both (A) and [B] sites.

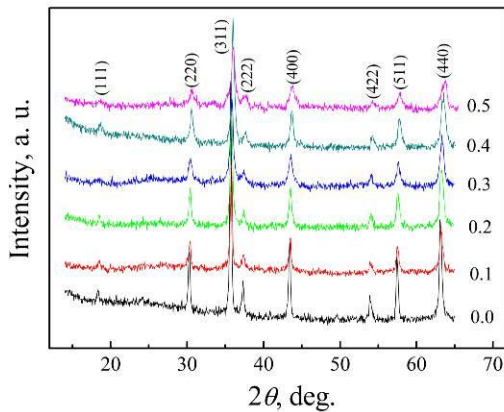


Fig. 1 – X-ray spectra of Ni-Cr ferrite powders

Table 1 – Structural parameters calculated from XRD patterns of the $\text{NiCr}_x\text{Fe}_{2-x}\text{O}_4$

x	a , nm	M , g mol^{-1}	d_x , g cm^{-3}	Cation distribution
0.0	0.8343	234.38	5.360	$(\text{Fe}_{1.0})[\text{Ni}_{1.0}\text{Fe}_{1.0}]\text{O}_4$
0.1	0.8337	233.99	5.363	$(\text{Fe}_{1.0})[\text{Ni}_{0.9}\text{Cr}_{0.1}\text{Fe}_{1.0}]\text{O}_4$
0.2	0.8330	233.61	5.367	$(\text{Fe}_{1.0})[\text{Ni}_{0.8}\text{Cr}_{0.2}\text{Fe}_{1.0}]\text{O}_4$
0.3	0.8323	233.22	5.372	$(\text{Fe}_{1.0})[\text{Ni}_{0.7}\text{Cr}_{0.3}\text{Fe}_{1.0}]\text{O}_4$
0.4	0.8316	232.84	5.376	$(\text{Fe}_{1.0})[\text{Ni}_{0.6}\text{Cr}_{0.4}\text{Fe}_{1.0}]\text{O}_4$
0.5	0.8306	232.45	5.387	$(\text{Fe}_{1.0})[\text{Ni}_{0.5}\text{Cr}_{0.5}\text{Fe}_{1.0}]\text{O}_4$

3.2 Particle Size and Deformation of Crystal

3.2.1. Definition of Integral Width of Line Taking into Account Ka-doublet

In order to determine the parameters of a nanostructure, the method of analyzing the integral width of diffraction lines is often used due to its simplicity, if instead of integral width, the width at half height of the maximum of diffraction lines is used [12]. However, there is a need to make some comments about using integral width and width at half height of the maximum of diffraction lines.

In general, extensions occur both at the expense of physical factors (the presence of micro-strains and areas of coherent scattering), and instrumental (geometric) factors (beam divergence, focusing). The influence of both factors, that is, physical and instrumental expansion, is in-additive, since each section of curve of the true diffraction expansion under the influence of the geometric conditions of the experiment is blurred by the same law $g(y)$. Mathematically, the extension of a line is described by a convolution operation:

$$h(x) = \int_{-\infty}^{+\infty} f(y)g(x-y)dy, \quad (1)$$

where $f(y)$ is the physical diffraction expansion function conditioned to the physical state of the sample, $h(x)$ and $g(y)$ are the intensity distribution function for the sample and the function that describes the hardware extension, respectively.

Analyzing the intensity distribution described by the expression (2), we can establish that the value of B is the extension of the line associated with β – the physical extension of the line and b – geometric extension of the line by expression:

$$B = \frac{\beta \cdot b}{\int g(x)f(x)dx}. \quad (2)$$

Here, B , b and β are the integral widths of the curves $h(x)$, $g(x)$ and $f(x)$

$$B = \int_{-\infty}^{+\infty} \frac{h(x)}{I_{\max}} dx, \quad b = \int_{-\infty}^{+\infty} \frac{g(x)}{I_{\max}} dx, \quad \beta = \int_{-\infty}^{+\infty} \frac{f(x)}{I_{\max}} dx \quad (3)$$

is the ratio of the area under the line to the maximum intensity I_{\max} .

Approximating the functions $g(x)$ and $f(x)$ in the form of the Cauchy (or Gaussian) function, relations are obtained for determining the true width of the diffraction

line: $B = b + \beta$ in the case of Cauchy or $B^2 = b^2 + \beta^2$ in the case of Gauss (approximation method).

A similar approach is also used to separate the effects of CSRs and micro-deformation. In the case where the expansion of the diffraction line is caused only by the micro-deformations, the integral line width is defined as

$$\beta_s = 4\varepsilon \operatorname{tg} \theta, \quad (4)$$

where ε is the mean value of the relative deformation module; when the extension is caused only by the size of the regions of coherent scattering, the integral width

$$\beta_D = \frac{k\lambda}{D \cdot \cos \theta}, \quad (5)$$

where D is the average linear size in the direction of CSRs of the normal to the reflecting plane, k is a constant equal to 0.9. When the extension is caused by the simultaneous influence of the micro-deformations and the CSR, then the integral width is defined as a Cauchy function

$$\beta_{hkl} = \beta_D + \beta_S. \quad (6)$$

It is worth noting that the convolution of the two Cauchy functions is not a Cauchy function, however, in most cases, it is believed that it is also close to the Cauchy function, which makes it possible to use the above-indicated separation.

Also, it should be noted that there is a difference between the half-width of the line w and its integral width β . In the case of the Cauchy function

$$\beta = \frac{\pi}{2} \cdot w, \quad (7)$$

and in the case of the Gaussian function:

$$\beta = \sqrt{\frac{\pi}{4 \ln 2}} \cdot w. \quad (8)$$

This difference also affects the defined microstructure parameters. In particular, the article [13] shows that the ratio of the dimensions of the blocks determined using the integral width to the dimensions of the blocks determined from the half width for the Cauchy function is equal to 0.71, and for the Gauss function – 1.06.

It is clear that this difference in the calculated sizes of blocks does not depend on the real size of the crystallite. Unfortunately, software developers do not mention these values in user guides, as well as in many articles where calculations are done manually. The result obtained in [13] showed that the peak profiles are close to the Lorentz form and, according to the recently published data [14], the experimental profile becomes close to the Lorentzian when about 70 % of the crystallites have dimensions in the range from half to two medium sizes.

Thus, when comparing the sizes of crystallites obtained by different researchers, it is necessary to take into account the method and methods by which they were determined. They must also be specified in the publications, or at least the name of the software that was used.

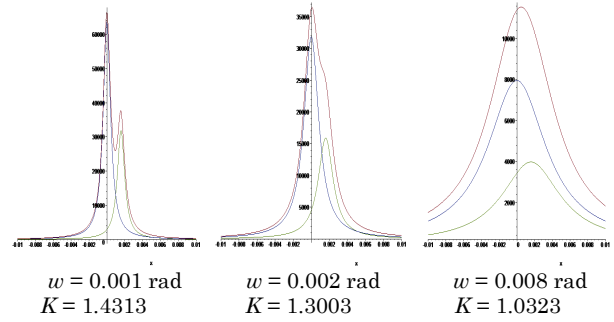


Fig. 2 – K_{α} -doublets for different line widths

The use of integral width also has the advantage in the presence of having a peak asymmetry. In this case, the separation of the K_{α} -doublet is essentially complicated. Therefore, when looking for the integral width of a line, it is necessary to take into account that the line can consist of two lines, that is K_{α} -doublet [15]. Therefore, there is a need to find out how much the existence of a doublet will affect the determination of microstructure parameters. For this, line was modeled by the Lorentz function:

$$y = \frac{2Aw}{\pi(w^2 + 4x^2)}. \quad (9)$$

Here, x is the angular variable, w is the width at the side of the maximum of lines, and A is the area below the line. The line a_2 was set to be exactly the same as the line a_1 , but with intensity two times smaller. Fig. 2 shows the effect of the doublet on the shape of the resulting line. As seen, the presence of a doublet can lead to a shift of the maximum of line. This can influence the calculated constant lattice of the compound determined without using of a full profile analysis.

To evaluate the effect of a doublet, the ratio of the integral width of the K_{α} -doublet β_{12} to the integral width β_1 of the line α_1 was calculated:

$$K = \frac{\beta_{12}}{\beta_1} = \frac{\int_{-\infty}^{\infty} \left(\frac{2Aw}{\pi(4x^2 + w^2)} + \frac{1}{2} \frac{2Aw}{\pi(4(x - \Delta x)^2 + w^2)} \right) dx / I_{\max 12}}{\int_{-\infty}^{\infty} \frac{2Aw}{\pi(4x^2 + w^2)} dx / I_{\max 1}} \quad (10)$$

where $I_{\max 12}$ is the maximum intensity of the doublet, $I_{\max 1}$ is the maximum of the intensity of the line α_1 , Δx is the angular distance between the lines α_1 and α_2 , which depends on the angle at which the doublet is placed. This angular distance was obtained by differentiating the Bragg formula with known wavelengths $K_{\alpha 1}$ and $K_{\alpha 2}$.

If the line width is small, then $K \approx 1.4$, when line width is large, then $K \approx 1$ and doublet can be ignored in this case. The coefficient K depends on the angle and line width, so K was determined in the range of line widths and angles that are in the X-ray diffraction analysis. The calculations were made using the program Maple, and their results for different angles on which doublet is located are shown in Fig. 3.

To make it more convenient to use this set of coefficients, the approximation of data was given. The next formula best describes this:

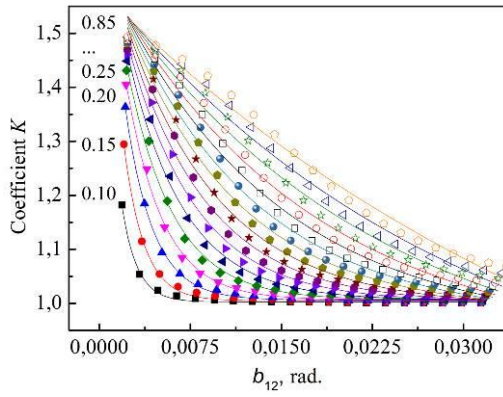


Fig. 3 – Approximate dependence of the coefficient K from the doublet width for different Bragg angles (from 0.10 rad to 0.85 rad with step 0.05 rad)

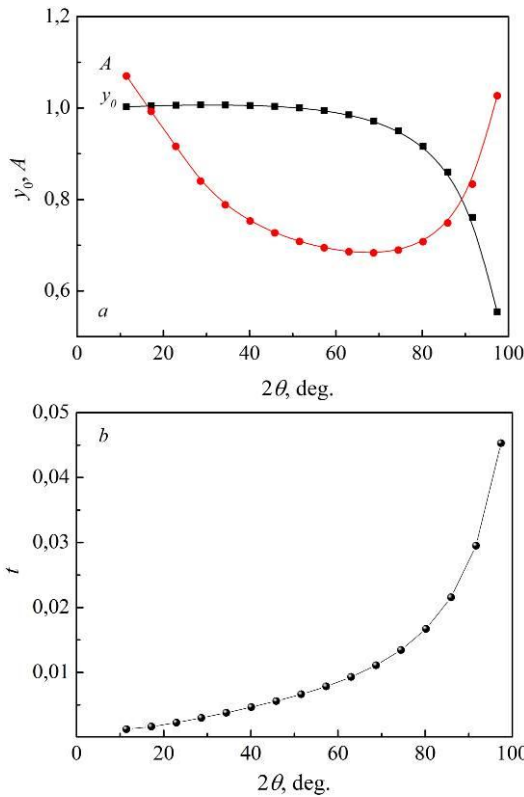


Fig. 4 – Approximate dependence of the coefficients y_0 , A and t from double Bragg angle

$$y = y_0 + Ae^{-\frac{x}{t}} \tag{11}$$

The dependence on the angle of the coefficients y_0 , A and t was approximated by polynomials (Fig. 4). As a result of approximation, the equations were obtained:

$$y_0 = 1.10452 - 0.01724 \cdot (2\theta) + 1.01 \cdot 10^{-3} \cdot (2\theta)^2 - 2.60759 \cdot 10^{-5} \cdot (2\theta)^3 + 3.04294 \cdot 10^{-7} \cdot (2\theta)^4 - 1/34285 \cdot 10^{-9} \cdot (2\theta)^5, \tag{12}$$

$$A = 1.12542 + 0.0055 \cdot (2\theta) - 1.3 \cdot 10^{-3} \cdot (2\theta)^2 + 3.77981 \cdot 10^{-5} \cdot (2\theta)^3 - 4.38885 \cdot 10^{-7} \cdot (2\theta)^4 + 1.85643 \cdot 10^{-9} \cdot (2\theta)^5, \tag{13}$$

$$t = -0.00668 + 0.00125 \cdot (2\theta) - 6.80105 \cdot 10^{-5} \cdot (2\theta)^2 + 1.79088 \cdot 10^{-6} \cdot (2\theta)^3 - 2.1197 \cdot 10^{-8} \cdot (2\theta)^4 + 9.44898 \cdot 10^{-11} \cdot (2\theta)^5. \tag{14}$$

We got K as a function of two variables $K = K(2\theta, \beta_{12})$, where 2θ is the double Bragg angle.

So, the integral width of $K_{\alpha 1}$ -line was getting by division the integral width of the K_{α} -doublet obtained from the experiments, by this coefficient K . This coefficient lets exactly and correctly to determine the parameters of the microstructure. Also, we should note that ignoring a doublet in determining the integral width leads to increase of the calculated block sizes by 6 %. All subsequent calculations were made taking into account the foregoing.

3.2.2. Debye-Scherrer Method

By means of Debye-Scherrer method, it is possible to divide the effects of expansion of diffraction lines, which are due to the small size of CSRs and micro-deformations. The XRD patterns of nickel-chromium powders were used to estimate the crystallite sizes. The average size of the CSRs of the studied samples was determined using the Debye-Scherrer formula (6).

It should be noted that the width of the Bragg peak also contributes to the instrumental width of the line [16], which is due to the width of the cracks limiting the bundle of X-rays, the difference in beam, the inaccuracy of setting the sample in its adapter. The average size of CSRs of powders was in the range 23-43 nm.

3.2.3. Williamson-Hall Method

In contrast to the Debye-Scherrer method, which uses only the average size of crystallites, the Williamson-Hall method allows to determine also the magnitude of the micro-deformation of the crystal lattice. This fundamental difference between these methods allows a division of the expand effects of the diffraction peaks associated with the size of the CSR and the micro-deformations. In this case, the dilatation related to the size of the crystallites (β_D) and the micro-deformation of the crystal lattice (β_S) is by the components of the total integral width of the Bragg reflex (7).

Then, using the Debye-Scherrer formula, we will write the expression (7) in the form:

$$\beta_{hkl} = \frac{k\lambda}{D \cos\theta} + 4\epsilon \tan\theta. \tag{15}$$

Multiplying the left and right parts of the last expression by $\cos\theta$, we get the following relation:

$$\beta_{hkl} \cos\theta = \frac{k\lambda}{D} + 4\epsilon \sin\theta. \tag{16}$$

The resulting equation is a representation of the so-called "Uniform Deformation Model" (UDM) [17], where it is believed that the deformations are uniform in all crystallographic directions taking into account the isotropic nature of the crystal, where the properties of the material do not depend on the direction, along which they are evaluated.

Fig. 5 shows the Williamson-Hall dependence in the coordinates $\beta_{hkl} \cos\theta$ ($4\sin\theta$), which is approximated by the linear function $y = A + Bx$. From the graphic dependence of $\beta_{hkl} \cos\theta$ ($4\sin\theta$), the average size of the CSRs was determined by extrapolating $\beta_{hkl} \cos\theta$ ($4\sin\theta$) to the value of $\sin\theta = 0$. The value of the micro-strains was found according to the dependence inclination (17) using the approximation parameters.

Fig. 5 shows that the inclination of approximating lines is different. This corresponds to different values of micro-deformation of crystal lattice. As a result of the calculations, it was found that the size of CSR in powders is within the range of 24-43 nm. We can state that in the NiCr_xFe_{2-x}O₄ ferrite, the size of CSRs decreases. The calculated value of micro-deformations in the samples varies from $4.23 \cdot 10^{-4}$ to $1.02 \cdot 10^{-3}$. However, Fig. 5 shows that the points relative to the approximated line have a large spread. This is a sign that, in the used model, some other parameters of the studied powders are obviously not yet taken into account. Therefore, the size-strain plot (SSP) method was used, which takes into account the form of particles.

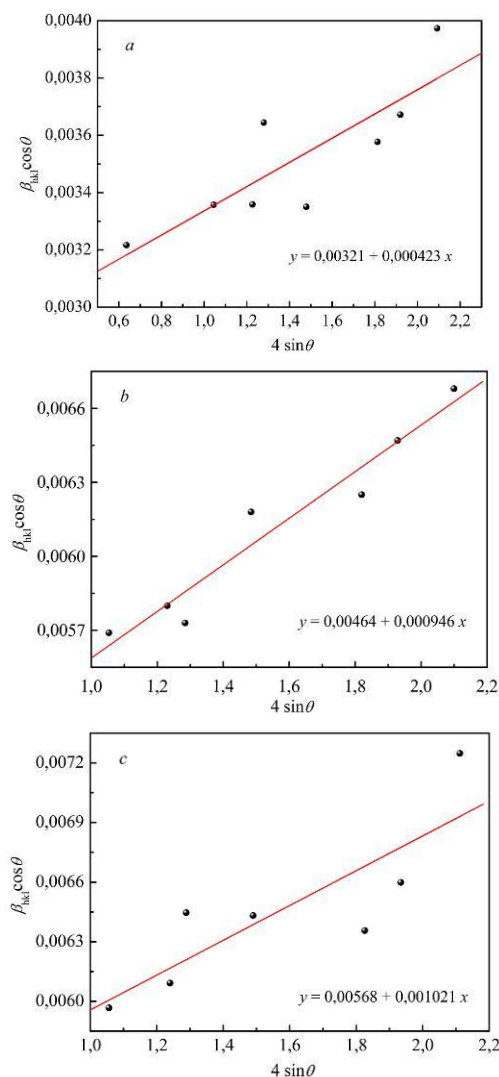


Fig. 5 – The Williamson-Hall analysis of nanoparticles according to the UDM model: *a* – NiFe₂O₄, *b* – NiCr_{0.3}Fe_{1.7}O₄ and *c* – NiCr_{0.5}Fe_{1.5}O₄

3.2.4. SSP Method

In determining the size of the CSRs and the micro-deformation values of nickel-chromium ferrites by the Williamson-Hall method, it was considered that the deformations are uniform in all crystallographic directions. For the case of an isotropic nature of crystals, the estimation of the above parameters also can be obtained by

using a linear plot of SSP method that has an advantage over other methods, since the accuracy of the diffraction reflexes data at high angles is usually low. In this approximation, the reflex extension due to the particle size can be described using the Lorentz function, and the expansion of the reflex due to the micro-deformations of the crystal lattice – the Gaussian function. Taking into account the above, we obtain the following expression:

$$(d_{hkl}\beta_{hkl} \cos \theta / \lambda)^2 = \frac{K}{D} (d_{hkl}^2 \beta_{hkl} \cos \theta / \lambda) + (2\varepsilon)^2, \quad (17)$$

where K is a constant, which depends on the particles shape (it is $3/4$ for the spherical form of the particles).

Fig. 6 shows the dependence $(d_{hkl}\beta_{hkl} \cos \theta / \lambda)^2$ of $(d_{hkl})^2 \beta_{hkl} \cos \theta / \lambda$, which is approximated by the linear function $y = A + Bx$. In this case, the size of the CSRs of NiCr_xFe_{2-x}O₄ powders is determined by the inclination of the approximating line, and the value of the micro-deformations is determined according to the formula $\varepsilon = 0.5\sqrt{A}$.

The results obtained using the Debye-Scherrer formula, Williamson Hall and SSP methods are given in Table 2. According to tabular data, the average sizes of CSRs are little different from each other. It should be noted that when analyzing the average size of particles by the Williamson-Hall method, there is a larger scatter of experimental points than the SSP method.

In the case of micro-deformations, for all powders of the studied system, the values of ε obtained using the SSP method are significantly bigger than the values of the micro-deformations determined by the Williamson-Hall method and are within the range from $4.69 \cdot 10^{-4}$ to $2.69 \cdot 10^{-3}$.

However, taking into account the distribution of experimental points from the approximated lines by the Williamson-Hall method, the obtained results of micro-deformation values calculated according to the SSP method are more trued, since all experimental points are on the straight line.

Table 2 – Geometric parameters of nickel-chromium ferrites

x	Debye-Scherrer formula	Williamson-Hall method		SSP method	
	D , nm	D , nm	ε	D , nm	ε
0.0	43	43	$4.23 \cdot 10^{-4}$	42	$4.69 \cdot 10^{-4}$
0.1	35	38	$5.14 \cdot 10^{-4}$	32	$5.47 \cdot 10^{-4}$
0.2	32	35	$5.72 \cdot 10^{-4}$	31	$7.83 \cdot 10^{-4}$
0.3	26	30	$9.46 \cdot 10^{-4}$	25	$8.50 \cdot 10^{-4}$
0.4	29	29	$9.55 \cdot 10^{-4}$	24	$1.78 \cdot 10^{-3}$
0.5	23	24	$1.02 \cdot 10^{-3}$	19	$2.69 \cdot 10^{-3}$
Δ	± 2	± 3	$\pm 5 \cdot 10^{-5}$	± 1	$\pm 2 \cdot 10^{-5}$

3.3 Morphology Study

Typical morphologies of NiCr_xFe_{2-x}O₄ particles visualized by SEM are shown in Fig. 7. A distribution of particle diameters, volumes, or numbers can be obtained from a study of the micrograph. The prepared particles are nanosized and nearly spherical in shape. The distribution of NiFe₂O₄ particles obtained from SEM is shown as the histogram in Fig. 8 and consists of a combination of nanodispersed particles.

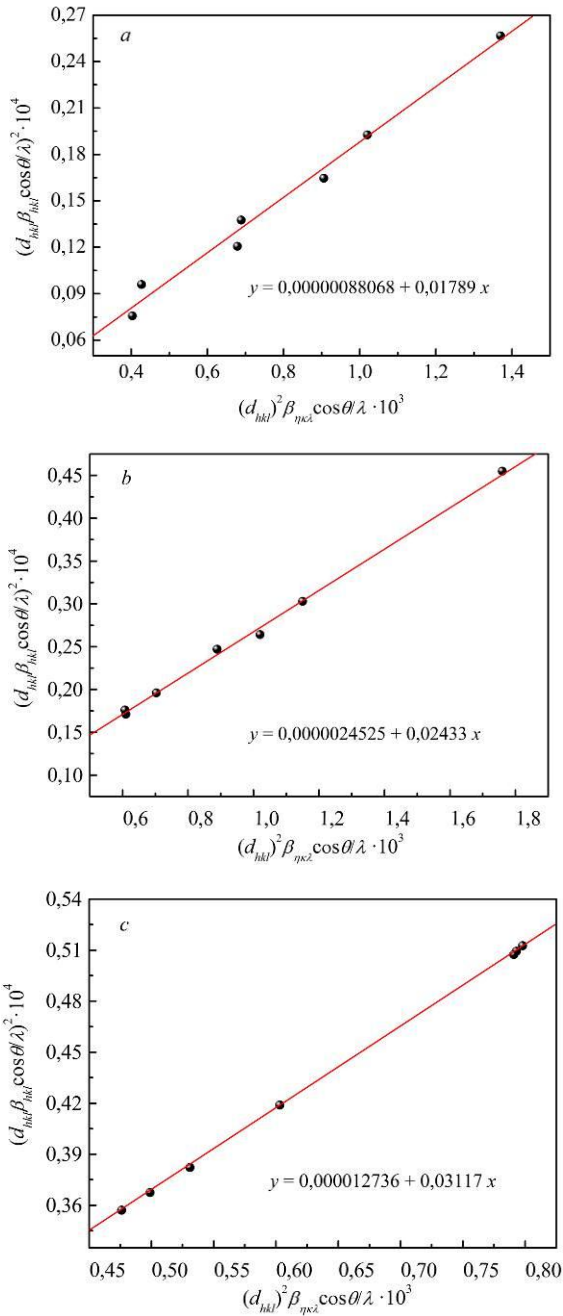


Fig. 6 – The SSP plot of nickel-chromium ferrites: *a* – NiFe₂O₄, *b* – NiCr_{0.2}Fe_{1.8}O₄, *c* – NiCr_{0.4}Fe_{1.6}O₄

By least-square fitting to a Gaussian normal distribution, the particle size distribution may be analyzed. However, it is confirmed that the size distribution of particles is not normal but lognormal [18].

The lognormal distribution $f(\ln x)$ is represented as follows:

$$f(\ln x)d(\ln x) = \frac{\exp(-(\ln x - \overline{\ln x})^2 / 2\sigma^2)}{\sqrt{2\pi}\sigma} d\ln x, \quad (18)$$

where x is the diameter of the particles, σ is the standard deviation of $\ln x$ and $\overline{\ln x}$ is the mean of the $\ln x$. If x_m is the median of x and $\overline{\ln x} = \ln(x_m)$, we get:

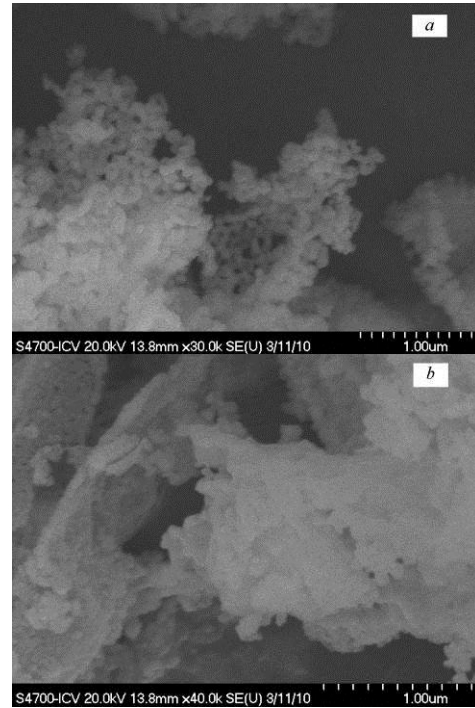


Fig. 7 – SEM micrograph of Ni-Cr ferrites: *a* – NiFe₂O₄ and *b* – NiCr_{0.5}Fe_{1.5}O₄

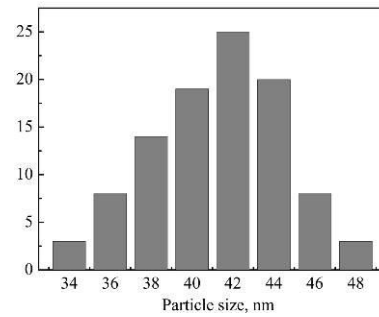


Fig. 8 – The particle analyzer histogram of NiFe₂O₄

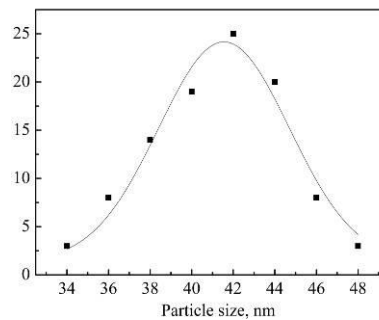


Fig. 9 – The least-square fit of the lognormal distribution of particles

$$f(x)dx = \frac{\exp(-\ln(x/x_m)^2 / 2\sigma^2)}{\sqrt{2\pi}\sigma x} dx, \quad (19)$$

The least-square fit of the lognormal distribution to the measured points obtained by the SEM micrographs is shown in Fig. 9. The average particle size of NiFe₂O₄ was found in the range 41–42 nm. This average particle size agrees nearly with the value of 42–43 nm estimated from the X-ray powder diffraction peaks.

4. CONCLUSIONS

In summary, the NiCr_xFe_{2-x}O₄ nanopowders were successfully synthesized by the SGA technology. The single-phase powders with a cubic structure of spinel space group Fd3m were obtained. The lattice parameter decreases from 0.8343 nm to 0.8306 nm because the replacement of larger ionic crystal radius of Fe³⁺ by smaller Cr³⁺ occurs. As the concentration of Cr³⁺ cations increases in the composition of the ferrites, the X-ray density increases linearly. The Ni²⁺ and Cr³⁺ cations occupy exclusively the B-site, while the Fe³⁺ cations occupy the A and B-sites.

The XRD patterns were analyzed by the Scherrer formula, Williamson-Hall and the SSP methods. Systematic substitution of Cr³⁺ ions resulted in decrease

of nanoparticle sizes from 43 nm to 23 nm for NiFe₂O₄ and NiCr_{0.5}Fe_{1.5}O₄, respectively, which were obtained by Scherrer formula. It is established that the determined particle size of the powders according to the SSP method is in the range of 19-42 nm. The particle size obtained by Williamson-Hall method is slightly higher than those obtained by other methods. This is due to the scattering of experimental points from the approximated line by the Williamson-Hall method.

Analyzing the resulting graphic dependences of the above models, we can conclude that the result obtained by the SSP model is the most accurate because all experimental points are on the straight line. The SEM results are in good agreement with the results of the SSP methods.

REFERENCES

1. V.S. Bushkova, B.K. Ostafiychuk, *Powder Metall. Metal Ceram.* **54**, 509 (2016).
2. J.G.M. Van Berkum, R. Delhez, Th.H. Keijsers, E.J. Mittemeijer, *Acta Cryst.* **52**, 730 (1996).
3. K. Ramakanth, *Basic of Diffraction and Its Application* (I.K. International Publishing House Pvt. Ltd: New Dehli: 2007).
4. J. Zhang, Y. Zhang, K. W. Xu, V. Ji, *Solid State Commun.* **139**, 87 (2006).
5. S. Singhal, J. Singha, S.K. Barthwal, K. Chandraa, *J. State Chem.* **178**, 3183 (2005).
6. V.S. Bushkova, B.K. Ostafiychuk, I.P. Yaremij, M.L. Mokhnatskiy, *Metallofiz. Nov. Tekhnol.* **38**, 601 (2016).
7. V.S. Bushkova, *J. Nano-Electron. Phys.* **7**, 03021 (2015).
8. V.S. Bushkova, *Low Temp. Phys.* **43**, 1724 (2017).
9. Vira S. Bushkova, Ivan P. Yaremij, *J. Magn. Magn. Mater.* **461**, 37 (2018).
10. S.H. Lee, S.J. Yoon, G.J. Lee, H.S. Kim, C.H. Yo, K. Ahn, D.H. Lee, K.H. Kim, *Mater. Chem. Phys.* **61**, 147 (1999).
11. V.S. Bushkova, I.P. Yaremij, R.P. Lisovsky, B.V. Karpyk, *J. Nano-Electron. Phys.* **9**, 02011 (2017).
12. R. Yogamalar, R. Srinivasan, A. Vinu, K. Ariga, A.C. Bose, *Solid State Commun.* **149**, 1919 (2009).
13. V. Uvarov, I. Popov, *Mater. Charact.* **85**, 111 (2013).
14. Hosokawa Masuo, Nogi Kiyoshi, Naito Mario, Yokogama Togokazu, *Nanoparticle technology handbook* (Elsevier: The Netherlands: 2012).
15. I. Yaremij, S. Yaremij, V. Fedoriv, O. Vlasii, A. Lucas, *Eastern-European Journal of Enterprise Technologies* **5** No 5 (95), 61 (2018).
16. K.D. Rogers, P. Daniels, *Biomaterials* **23**, 2577 (2002).
17. T. Prabhu, K.V. Rao, V.S.S. Kumar, B.S. Kumari, *World J. Nano Scien. Engin.* **4**, 21 (2014).
18. Yangkyu Ahn, Eun Jung Choi, *J. Korean Phys. Soc.* **41**, 123 (2002).

X-променеви аналіз наночастинок NiCr_xFe_{2-x}O₄ з використанням Дебая-Шеррера, Вільямсона-Холла і графічного розмірно-деформаційного методів

І.П. Яремій¹, В.С. Бушкова¹, Н.І. Бушков¹, С.І. Яремій²

¹ ДВНЗ «Прикарпатський національний університет імені Василя Стефаника», вул. Шевченка, 57, 76025 Івано-Франківськ, Україна

² Івано-Франківський національний медичний університет, вул. Галицька, 2, 76018 Івано-Франківськ, Україна

Метою роботи є створення та вивчення наночастинок NiCr_xFe_{2-x}O₄, використовуючи золь-гель метод за участю автогоріння (ЗГА). Після завершення процесу автогоріння було отримано фазу, яка відповідає кубічній структурі просторової групи шпінелі Fd3m. Встановлено залежність параметра ґратки та густини X-променевого випромінювання порошоків феритів від вмісту нікелю. Величина параметра ґратки зменшуються від 0.8343 нм до 0.8306 нм із збільшенням вмісту іонів Cr³⁺. Зменшення параметра ґратки за рахунок збільшення концентрації Cr можна пояснити заміною більшого іонного радіуса Fe³⁺ меншим іонним радіусом Cr³⁺. X-променева густина dx зростає від 5.360 г см⁻³ до 5.387 г см⁻³ внаслідок збільшенні ступеня заміщення x. Дослідження розподілу катіонів вказує на те, що іони нікелю та хрому мають тенденцію займати октаедричні позиції, тоді як іони заліза мають тенденцію займати як тетраедричні, так і октаедричні підґратки. Морфологічні спостереження показують, що розмір частинок значно зменшується зі збільшенням вмісту Cr, а розмір частинок стає більш однорідним. Розмір частинок і мікродеформації кристалічної ґратки були розраховані за шириною X-променевого профілю та кута. Інтегральну ширину Ka₁-лінії одержано за допомогою поділу інтегральної ширини Ka-дублету, отриманого з експерименту, за коефіцієнтом K. Визначаючи інтегральну ширину, ігнорування дублету призводить до збільшення розрахункових розмірів блоку на 6 %. Розміри частинок порошоків NiCr_xFe_{2-x}O₄ проаналізовано за допомогою формули Шеррера, методу Вільямсона-Холла та розмірно-деформаційного методу. Визначаючи середній розмір часток методом Вільямсона-Холла (24-43 нм), спостерігається більший розкид експериментальних точок від апроксимаційної прямої, ніж за розмірно-деформаційним методом (19-42 нм). Заміщення іонами Cr³⁺ призводить до

зменшення розмірів наночастинок. Значення мікродеформацій ϵ , отриманих методом SSP, знаходяться в діапазоні від $4.69 \cdot 10^{-4}$ до $2.69 \cdot 10^{-3}$. Середній розмір частинок NiFe_2O_4 знайдено за найменшим квадратичним логарифмічним розподілом виміряних точок, отриманих з використанням даних СЕМ. Виявлено, що середній розмір частинок знаходиться в діапазоні 41-42 нм.

Ключові слова: Ферит, Нанопорошок, Золь-гель автогоріння, X-променевий аналіз, Мікродеформація.